〈Technical Note〉

A DYNAMIC SIMULATION OF THE SULFURIC ACID DECOMPOSITION PROCESS IN A SULFUR-IODINE NUCLEAR HYDROGEN PRODUCTION PLANT

YOUNGJOON SHIN*, JIWOON CHANG, JIHWAN KIM, BYUNGHEUNG PARK, KIYOUNG LEE, WONJAE LEE and JONGHWA CHANG
Korea Atomic Energy Research Institute
1045 Daedeok-daero, Yuseong-gu, Daejeon, 305-353, Korea
*Corresponding author. E-mail : nyjshin@kaeri.re.kr

Received August 11, 2008
Accepted for Publication March 27, 2009

In order to evaluate the start-up behavior and to identify, through abnormal operation occurrences, the transient behaviors of the Sulfur Iodine(SI) process, which is a nuclear hydrogen process that is coupled to a Very High Temperature Gas Cooled Reactor (VHTR) through an Intermediate Heat Exchanger (IHX), a dynamic simulation of the process is necessary. Perturbation of the flow rate or temperature in the inlet streams may result in various transient states. An understanding of the dynamic behavior due to these factors is able to support the conceptual design of the secondary helium loop system associated with a hydrogen production plant. Based on the mass and energy balance sheets of an electrodialysis-embedded SI process equivalent to a 200 MW_{th} VHTR and a considerable thermal pathway between the SI process and the VHTR system, a dynamic simulation of the SI process was carried out for a sulfuric acid decomposition process (Second Section) that is composed of a sulfuric acid vaporizer, a sulfuric acid decomposer, and a sulfur trioxide decomposer. The dynamic behaviors of these integrated reactors according to several anticipated scenarios are evaluated and the dominant and mild factors are observed. As for the results of the simulation, all the reactors in the sulfuric acid decomposition process approach a steady state at the same time. Temperature control of the inlet helium is strictly required rather than the flow rate control of the inlet helium to keep the steady state condition in the Second Section. On the other hand, it was revealed that the changes of the inlet helium operation conditions make a great impact on the performances of SO_3 and H_2SO_4 decomposers, but no effect on the performance of the H_2SO_4 vaporizer.

KEYWORDS : Nuclear Hydrogen, VHTR, Hydrogen Production, SI Process, NHDD, Dynamic Simulation, Thermal Pathway

1. INTRODUCTION

A Sulfur-Iodine (SI) process that requires high temperature energy is well known as a feasible technology to produce hydrogen from water [1]. The SI process for hydrogen production requires sufficient heat that can be supplied by nuclear reactors. A very high temperature gas cooled reactor (VHTR) should be used as a high temperature energy source. The VHTR-SI hydrogen production system consists of the nuclear reactor, primary and secondary helium cooling systems, and SI process. The helium in the secondary cooling system acts as a medium to transfer the high temperature energy to the SI process.

The hydrogen production by the SI process coupled to the VHTR through an intermediate heat exchanger (IHX) is achieved by the following three chemical reactions while iodine and sulfur dioxide are recycled throughout the process.

$$I_2 + SO_2 + 2H_2O \rightarrow 2HI + H_2SO_4\ (\sim 120℃)\text{: Exothermic Bunsen reaction} \quad (1)$$

$$H_2SO_4 \rightarrow H_2O + SO_2 + 1/2O_2\ (\sim 850℃)\text{: Endothermic reaction} \quad (2)$$

$$2HI \rightarrow H_2 + I_2\ (300 \sim 400℃)\text{: Endothermic reaction} \quad (3)$$

Process heat exchanging (PHE) modules equipped with a H_2SO_4 vaporizer and a H_2SO_4 decomposer for the chemical reaction represented by Eq. (2) and with a HI decomposer for the chemical reaction represented by Eq. (3) are required in the SI process. The high temperature thermal energy is transferred to these chemical reactors through the PHE modules by the secondary helium coolant, and then it returns to the IHX to recharge the thermal energy from the VHTR.

Candidate nuclear hydrogen development and demonstration (NHDD) plant designs based on a 200 MW_{th} VHTR core and a SI thermochemical process are being studied by the Korea Atomic Energy Research Institute (KAERI) [2]. In connection with this, KAERI conceptually studied how to construct a secondary helium pathway through the PHE modules and proposed a secondary helium pathway (draft) in 2007 based on the mass and energy balance of the KAERI SI process using a 200 MW_{th} VHTR [3].

Even though a dynamic leading study on this system is required in order to prepare a conceptual flow diagram of the coupling system, limited information was introduced by the JAEA research team [4].

Many studies on dynamic simulations of a shell-and-tube heat exchanger have been performed by using a multicell dynamic model or a dispersion model [5,6]. Dynamic studies on the vaporization of a solution have mainly focused on multi-effect evaporators to understand a system start-up, shut-down, and troubleshooting, in which a plant's performance changes significantly [7,8].

In this study, a thermal pathway between the secondary helium line and the SI process is introduced. A dynamic simulation model based on the H_2SO_4 vaporizer and decomposer of the SI process has been established and applied to analyze the start-up and transient behaviors.

The purposes of this paper are as follows: (1) to evaluate the start-up behavior of the H_2SO_4 vaporizer and decomposer connected in series and (2) to identify the effect of the inlet helium condition that was changed suddenly from the normal operation temperature and flow rate during their transient performances.

2. SYSTEM DESCRIPTION

A nuclear hydrogen production system is composed of a VHTR, an IHX, and a SI process, as shown in Fig 1. Helium is used as a high temperature energy carrier gas between the VHTR and the IHX or the IHX and the SI process.

The SI process consists of 3 parts, i.e. a Bunsen reaction part (First Section), a sulfuric acid concentration and decomposition part (Second Section), and a hydrogen iodide concentration and decomposition part (Third Section).

The key chemical reactor in the First Section is a Bunsen reactor which has not only the function of the Bunsen reaction of Eq. (1), but also the function of a mutual separation of the immiscible sulfuric acid and hydrogen iodide phases generated from the Bunsen reaction, a sulfuric acid stripper to remove the residual sulfuric acid from the separated hydrogen iodide phase, and a sulfur dioxide scrubber to recover the sulfur dioxide from the oxygen/sulfur dioxide mixture. These reactors do not need to attain thermal energy from an external thermal source.

The Second Section consists of the first and second sulfuric acid distillation columns, a sulfuric acid vaporizer, a sulfuric acid decomposer, and a sulfur trioxide decomposer. All of the chemical reactors need a heat supply from an external heat source. When an array of these reactors is determined by the operational temperature order, the high temperature helium to heat these reactors has to go through the sulfur trioxide, sulfuric acid decomposers, and the vaporizer in series. The cooled helium vented from the vaporizer is recycled to the intermediate heat exchanger to receive thermal energy. On the other hand, the sulfuric acid distillation columns that operate at a lower temperature can be heated by the sensible and latent heats of the process gas, as shown in Fig. 2. Sometimes we have to use a heat pump to maximize the heat utilities.

The Third Section has a HIx solution distillation column for an additional concentration of the HIx solution that is discharged from electrodialysis equipment that is to preliminarily concentrate the HIx solution by using the cationic membrane in an electric field. This electrodialysis equipment is not presented in Fig. 2 because it is operated at room temperature. A membrane reactor which is a key piece of equipment in the Third Section has two functions of catalysis decomposition of HI and preferential separation of hydrogen from the decomposed gas mixture of $H_2/I_2/$

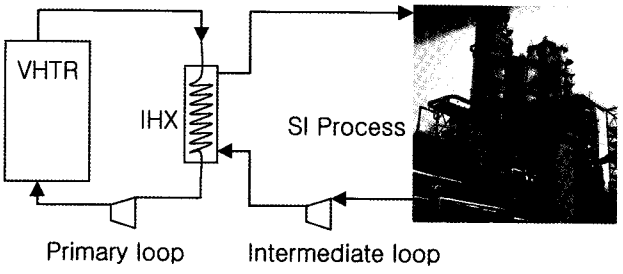

Fig. 1. Nuclear Hydrogen Production System

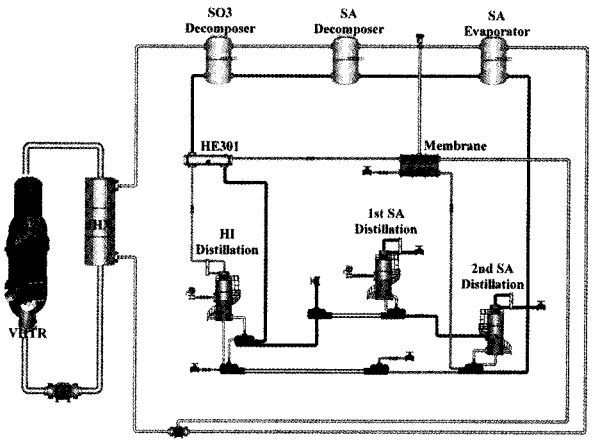

Fig. 2. Thermal Pathway of the SI Process Coupled to a VHTR

HI /H_2O. The membrane reactor is heated by the circulated helium, and the HI_x distillation column is heated by the sensible heat of another process gas. However, the electrodialysis equipment is operated at room temperature.

3. DYNAMIC SIMULATION MODEL

3.1 Mathematical Modeling of a H_2SO_4 Vaporizer

A short tube vertical evaporator was selected as the vaporizer of the 98 wt% H_2SO_4 solution, which is near azeotropic composition in the Second Section of the SI process. We can establish the following mathematical models by assuming that the aqueous phase in the vaporizer vessel is homogeneous at uniform temperature.

If $T_{aq,in} \leq T < T_b$,

$$\rho c_p V \frac{dT}{dt} = UA\left(\frac{T_{He,in} + T_{He,out}}{2} - T\right) \tag{4}$$

$$T_{He,out}(t) = \{\left(\frac{F_{He}c_{p,He}}{UA} - \frac{1}{2}\right)T_{He,in} + T(t)\} / \left(\frac{F_{He}c_{p,He}}{UA} + \frac{1}{2}\right) \tag{5}$$

If $T=T_b$,

$$Q = UA\Delta T_{lmtd} \tag{6}$$

$$\Delta T_{lmtd} = \frac{T_{He,in} - T_{He,out}}{\ln \dfrac{(T_{He,in} - T_b)}{(T_{He,out} - T_b)}} \tag{7}$$

$$\omega = Q / \lambda \tag{8}$$

Where, ρ (kg-mol/m^3) and c_p (kJ/(kg-mol K)) are the molar density and heat capacity of the 98 wt% H_2SO_4 solution, V (m^3) is the effective volume of the vaporizer charged by the sulfuric acid solution, $T_{aq,in}$ (K) is the temperature of the inlet sulfuric acid solution, T (K) is the average temperature of the sulfuric acid solution in the vaporizer, T_b (K) is the boiling point of the 98 wt % sulfuric acid solution at a given operation pressure, $T_{He,in}$ (K) and $T_{He,out}$ (K) are the helium inlet and outlet temperatures at the vaporizer, $c_{p,He}$ (kJ/(kg-mol K)) and F_{He} (kg-mol/s) are the heat capacity and molar flow rate of the helium, U (kJ/(m^2 s K)) is the over-all heat transfer coefficient, A (m^2) is the total heat transfer area of the vaporizer, and λ (kJ/kg-mol) and ω (kg-mol/s) are the latent heat and vaporization rate of the 98 wt% H_2SO_4 solution.

3.2 Mathematical Modeling of a H_2SO_4 Decomposer

The decomposition of H_2SO_4 in the SI process takes place in the forward and backward directions simultaneously as follows.

$$H_2SO_4 = SO_3 + H_2O \tag{9}$$

This is an endothermic chemical reaction, and the required energy is transmitted from a primary energy source, such as a VHTR.

From the viewpoints of thermodynamic equilibrium and kinetics, a higher operation temperature insures a higher decomposition yield. At reaction temperature T (K), a reactant-based chemical reaction rate ($-r_{H_2SO_4}$) for Eq. (9) can be expressed as follows [9,10].

$$-r_{H_2SO_4} = r_{SO_3} = r_{H_2O} = k_f\{\frac{C_{H_2SO_4,in}(1-X)}{(1+\varepsilon X)}\frac{T_{in}}{T} - \frac{1}{K_c}\frac{C_{H_2SO_4,in}(M+X)}{(1+\varepsilon X)}\frac{T_{in}}{T}\} \tag{10}$$

$$k_f = 2.9812\times10^7 \exp(-1.0570\times10^4 / T) \tag{11}$$

$$K_c = 1554.1 - 7.512T + 1.105\times10^{-2}T^2 - 2.450\times10^{-7}T^3 - 1.178\times10^{-8}T^4 + 7.182\times10^{-12}T^5 \tag{12}$$

$$M = \frac{C_{SO_3,in}}{C_{H_2SO_4,in}} \tag{13}$$

Where, k_f (s^{-1}) is the forward reaction constant of Eq. (9), X is the conversion fraction of H_2SO_4, $C_{H_2SO_4,in}$ (mol/m^3) and $C_{SO_3,in}$ are the inlet concentrations of H_2SO_4 and SO_3, T_{in} (K) is the inlet temperature of the process gases, and K_c is the equilibrium constant of Eq. (9). A volumetric expansion factor (ε) due to the decomposition of H_2SO_4 in Eq. (10) has a unique value of 0.2471.

The process gas in the tube side of a shell-and-tube type H_2SO_4 decomposer is heated by the high temperature helium in the shell side of the decomposer. The process gas and the helium stream maintain a count-current flow in the tube and shell sides, respectively. The decomposition of H_2SO_4 takes place inside the tube, and this chemical reaction requires a proper volume to maintain a sufficient residence time.

Based on this type of decomposer, we can establish the following mass and energy balances in a differential volume of the tube side from a longitudinal length L to L+dL at a differential time.

$$-\frac{\partial F_{H_2SO_4}}{\partial V_{RX}} - (-r_{H_2SO_4}) = \frac{\partial C_{H_2SO_4}}{\partial t} \tag{14}$$

$$Ua(T_{He} - T_{H_2SO_4}) - \sum_i F_i c_{p,i}\frac{\partial T_{H_2SO_4}}{\partial V_{RX}} + (-r_{H_2SO_4})(-\Delta H_{RX}) = \sum_i C_i c_{p,i}\frac{\partial T_{H_2SO_4}}{\partial t} \tag{15}$$

Where, F_{H2SO4} (mol/s) is the molar flow rate of H_2SO_4, V_{RX} (m^3) is the reactor volume, C_{H2SO4} (mol/m^3) is the molar concentration of H_2SO_4 in the reactor, t (s) is the operation time, a (m^2/m^3) is the heat transfer area across the wall of the tube per tube volume, T_{He} (K) and T_{H2SO4} (K) are the fluid temperatures of the helium and H_2SO_4, respectively, F_i (mol/s) is the molar flow rate of the i_{th} component, $c_{p,i}$ (kJ/(mol K)) is the heat capacity of the i_{th} component, ΔH_{RX} (kJ/mol) is the heat of the H_2SO_4 decomposition, and C_i (mol/m^3) is the molar concentration of the i_{th} component in the reactor.

A heat balance between the shell side stream (He) and the tube side stream (process gases including H_2SO_4) can be established as follows.

$$Ua(T_{He,j} - T_{H_2SO_4,j}) = F_{He} c_{p,He} (T_{He,j+1} - T_{He,j}) \quad (16)$$

Where, F_{He} is the molar flow rate of He. The overall heat transfer coefficient (U), which includes individual terms, is given by the following equation [11].

$$\frac{1}{U} = \frac{1}{h_o} + \frac{1}{h_i (D_i / D_o)} + \frac{1}{h_w} + \frac{1}{h_s} \quad (17)$$

$$h_i = \frac{0.023 c_{p,i} G_i}{(c_{p,i}\mu_i / \lambda_i)^{2/3} (D_i G_i / \mu_i)^{0.2}} \quad (18)$$

$$h_o = \frac{0.273 c_{p,He} G_{He}}{(c_{p,He}\mu_{He} / \lambda_{He})^{2/3} (D_o G_{He} / \mu_{He})^{0.365}} \quad (19)$$

$$h_w = \frac{2\lambda_t}{(D_o - D_i)} \quad (20)$$

Where, D_i (m) and D_o (m) are the inside and outside diameters of the tube, λ_i (kJ/(s m K)) and λ_t (kJ/(s m K)) are the heat conductivities of the gas phase and the tube material, and G_i (kg/(s m^2)) and μ_i (kPa s) are the mass flux and viscosity of the gas phase. The reported value of 5.670 kW·m^{-2}·K^{-1} for h_s due to a scaling was used [11].

3.3 Mathematical Modeling of a SO_3 Decomposer

The decomposition of SO_3 requires the highest temperature in the SI process, and it only takes place in the forward direction as follows.

$$SO_3 \rightarrow SO_2 + 1/2O_2 \quad (21)$$

This reaction can be also achieved by supplying high temperature energy from the primary energy source, i.e. a VHTR.

From the viewpoints of a thermodynamic equilibrium and kinetics, a higher temperature condition for the SO_3 decomposition is also required to achieve a higher conversion yield. In order to reduce a large kinetic barrier, generally some catalysts are used. This is a different point of the H_2SO_4 decomposer.

Based on the reactance of the SO_3 which is being consumed, a reaction rate ($-r_{SO_3}$) for Eq. (21) can be expressed by the following equation with a reaction rate constant of k_d (s^{-1}).

$$-r_{SO_3} = r_{SO_2} = 2r_{O_2} = k_d C_{SO_3} \quad (22)$$

$$k_d = A \exp(-E_a / RT) \quad (23)$$

Where, A (s^{-1}) and E_a (kJ/mol) in Eq. (23) are the pre-exponential factor and the activation energy, respectively, and are accepted as 6.81×10^4 s^{-1} and 73.1 kJ/mol, respectively. These values are taken from Huang and T-Raissi [12] who assumed these values for a SO_3 decomposition in a plug flow reactor packed by a catalyst WX-2. The reaction rate can be further arranged by adopting a non-isothermal gas phase reaction concept [13] and a resultant expression is obtained as follows:

$$-r_{SO_3} = k_d \frac{C_{SO_3,in}(1-X)}{(1+\varepsilon X)} \frac{T_{in}}{T}. \quad (24)$$

The volumetric expansion factor (ε) in Eq. (24) has a unique value of 0.2371 that results from a concentration change due to a chemical reaction.

The process gas in the tube side of a shell-and-tube type SO_3 decomposer is heated by the high temperature helium in the shell side of the decomposer. Catalyst granules are packed inside the tube. The process gas and helium streams maintain a count-current flow in the tube and shell sides, respectively. The decomposition of SO_3 takes place on the surface of the catalysts inside the tube and this chemical reaction requires a proper volume to maintain a sufficient contact time.

Based on this type of decomposer, we can establish the following mass and energy balances.

$$-\frac{\partial F_{SO_3}}{\partial V_{RX}} - (-r_{SO_3}) = \frac{\partial C_{SO_3}}{\partial t} \quad (25)$$

$$Ua(T_{He} - T_{SO_3}) - \sum_i F_i c_{p,i} \frac{\partial T_{SO_3}}{\partial V_{RX}} + (-r_{SO_3})(-\Delta H_{RX}) = \sum_i C_i c_{p,i} \frac{\partial T_{SO_3}}{\partial t} \quad (26)$$

Where, F_{SO3} is the molar flow rate of SO_3, V_{RX} is the

reactor volume, C_{SO3} is the molar concentration of SO_3 in the reactor, t is the operation time, a is the heat transfer area across the wall of the tube per tube volume, T_{He} and T_{SO3} are the fluid temperatures of the helium and SO_3, respectively, F_i is the molar flow rate of the i_{th} component, $c_{p,i}$ is the heat capacity of the i_{th} component, ΔH_{RX} is the heat of the SO_3 decomposition, and C_i is the molar concentration of the i_{th} component in the reactor.

A heat balance between the shell side stream (He) and the tube side stream (process gases including SO_3) can be established as follows.

$$Ua(T_{He,j} - T_{SO_3,j}) = F_{He} c_{p,He}(T_{He,j+1} - T_{He,j}) \quad (27)$$

Where, F_{He} is the molar flow rate of He. The overall heat transfer coefficient (U) in Eq. (27), which can be expressed by Eq. (17), has different individual heat transfer coefficients from Eqs. (18) and (19) because of the catalysts packed inside the tubes.

The equations for each heat transfer coefficient of a tube on the inside (h_i) and on the outside (h_o) are given in chemical engineering handbooks as Eqs.(28) [14], (29) [15], and (30) [11]. Two equations for a heat transfer coefficient on the inside of a tube can be applied with respect to a ratio of a catalyst's equivalent diameter (D_p) to the inside tube diameter (D_i).

$$h_i = 0.813\frac{\lambda_i}{D_i}\exp\left(-6D_p/D_i\right)\left(\frac{D_p G_i}{\mu_i}\right)^{0.9}, \quad \text{for } \frac{D_p}{D_i} < 0.35 \quad (28)$$

$$h_i = 0.125\frac{\lambda_i}{D_i}\left(\frac{D_p G_i}{\mu_i}\right)^{0.75}, \quad \text{for } 0.35 < \frac{D_p}{D_i} < 0.60 \quad (29)$$

$$h_o = \frac{0.273 c_{p,He} G_{He}}{(c_{pHe}\mu_{He}/\lambda_{He})^{2/3}(D_o G_{He}/\mu_{He})^{0.365}} \quad (30)$$

Where, λ_i is the heat conductivity of the gas phase, and G_i and μ_i are the mass flux and viscosity of the gas phase. The reported value of 5,670 $Wm^{-2}K^{-1}$ for h_s due to a scaling was used [11].

3.4 Integrated Simulation Model

The current dynamic simulation focuses on the consecutively connected SO_3 and H_2SO_4 decomposers and the vaporizer for a 90 mol% H_2SO_4 solution, which are placed in the Second Section, as shown in Fig. 3.

As shown in Fig. 3, the inlet helium temperature is 1,181 K, and the inlet temperature of the 90 mol% H_2SO_4 is 488 K. The operation pressure of the Second Section is

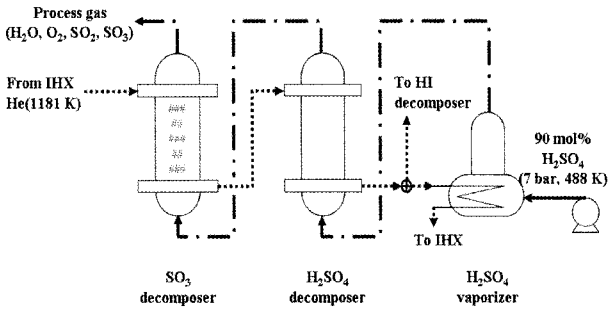

Fig. 3. Flow Sheet of the Second Section

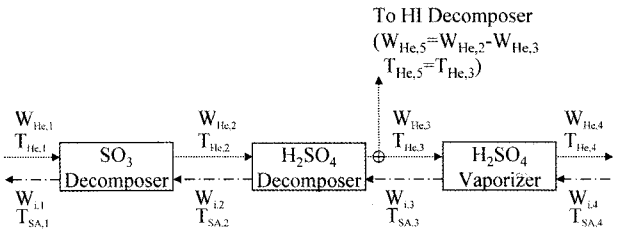

Fig. 4. Dynamic Simulation Model of the Second Section

Table 1. Equipment Specification and Parameters

Specification	H_2SO_4 Vaporizer	H_2SO_4 Decomposer	SO_3 Decomposer
Reactor type	Short tube vertical vaporizer	Shell & tube	Catalyst-packed tube & shell
Applied model	Macroscopic energy balance	Plug flow	Plug flow
Tube ID/OD(m)	0.013/0.016	0.013/0.016	0.013/0.016
Tube L(m)	2.496	2.123	3.206
# of tube	7560	2470	5440
Shell ID(m)	2.129	1.177	1.732
Shell L(m)	4.992 (including disengagement)	2.653 (including stationary head)	4.007 (including stationary head)
Heat transfer area(m^2)	752.5	208.9	695.5

7 bar. The helium of 1,181 K is introduced into the SO_3 decomposer, and the same mole flow rate is maintained at the H_2SO_4 decomposer. However, the outlet helium from the H_2SO_4 decomposer is introduced into two separated pipes: one is connected to the H_2SO_4 vaporizer and the other to the HI decomposer in the Third Section.

Based on this flow sheet, we can establish a simulation model as in Fig. 4.

Where, $W_{i,j}$ is a mole flow rate (mol/s) and $T_{i,j}$ is each stream temperature (K). The subscript 'i' means the components of He, H_2SO_4, SO_3, SO_2, H_2O, and O_2, respectively. The subscript 'j' means the stream position.

Each equipment specification used in our model simulation is shown in Table 1. The equipment sizing data is equivalent to a 200 MW_{th} VHTR-based SI process that has a hydrogen production rate of about 20,000 t•H_2/y.

4. SIMULATON AND RESULTS

A dynamic simulation was carried out to understand the start-up behavior of the Second Section of the SI process and to analyze the transient responses resulting from a disturbance of the variables for the helium inlet flow rate and temperature while approaching a steady state operation.

4.1 Start-up Behaviors

In the case of the start-up simulation, we assume that the helium of 1,181 K in the shell side and the inert gas inside the tubes are thermally equilibrated in both the H_2SO_4 and SO_3 decomposers at initial conditions. On the other hand, the inert gas inside the tubes and the sulfuric acid solution of 98 weight % H_2SO_4 and 2 weight % H_2O filled to the predetermined level in the short tube vertical vaporizer are initially maintained at 488 K due to closing a three-way valve to pass helium. The system operation is initiated by opening the three-way valve installed on the helium pipe line between the H_2SO_4 decomposer and the vaporizer. In this case, the normal flow rate conditions of the helium are 17,821.39 mol/s for $W_{He,1}$ and $W_{He,2}$ and 10,014.60 mol/s for $W_{He,3}$ and $W_{He,4}$, respectively. When the sulfuric acid in the vaporizer is heated up to the boiling point of the 90 mol% sulfuric acid solution at 7 bars by the helium of 1,181 K, a vapor equilibrated with the 90 mol% sulfuric acid solution is generated steadily and transferred to the sulfuric acid decomposer. At the same time, the metering pump is operated to continuously circulate the sulfuric acid solution of 488 K into the vaporizer.

Figs. 5 and 6 show the start-up behaviors of the temperature of helium and process streams at each position. The start-up behavior of the inlet and outlet compositions is shown in Fig. 7.

Based on the start-up behavior of the temperature and composition, it was confirmed that the reactors reached a steady state at the same time.

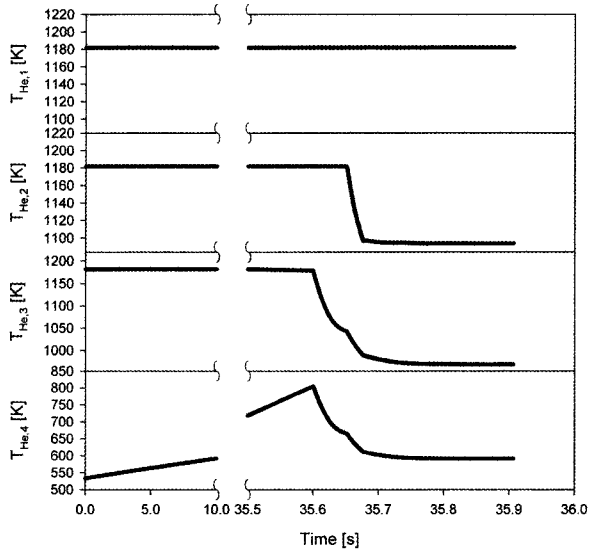

Fig. 5. Start-up Behavior of the Helium Temperature in each Position

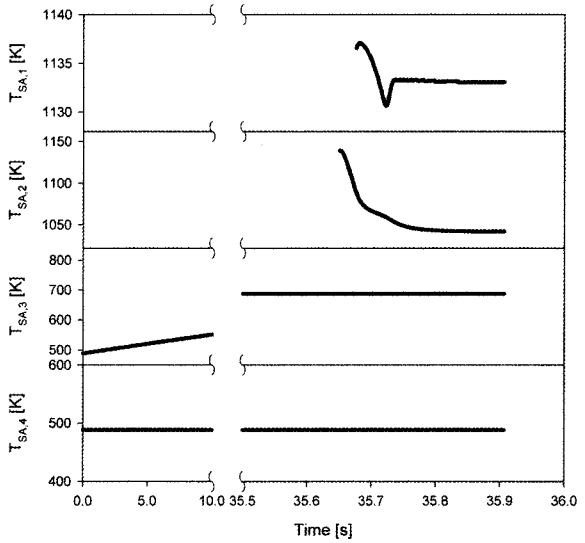

Fig. 6. Start-up Behavior of the Process Stream Temperature in each Position

4.2 Transient Responses on the Inlet Helium Temperature Disturbance

The transient responses of the process stream temperature and composition to the frequency forcing function of the inlet helium temperature were evaluated and their results are shown in Figs. 8 and 9.

As shown in Figs. 8 and 9, when the inlet helium temperature ($T_{He,1}$) is changed periodically within 1,181 $\pm$100 K, which is equivalent to a $\pm$8.5% disturbance based on a normal operation temperature of 1,181 K, the amplitude of $T_{SA,1}$ varies in the range of 1,045.2 K to

1,229.8 K, and in the range of 961.2 K to 1,117.4 K for $T_{SA,2}$. However, there is no perturbation of the temperature ($T_{SA,3}$) for the 90 mol% H_2SO_4 solution in the vaporizer.

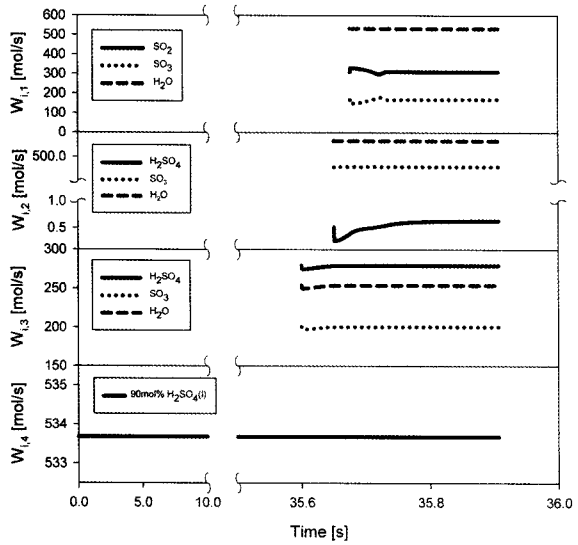

Fig. 7. Start-up Behavior of the Process Stream Composition in each Position

With respect to the composition, the maximum effect occurs at the sulfuric acid concentration ($W_{H2SO4,2}$) discharged from the H_2SO_4 decomposer. The amplitude of $W_{H2SO4,2}$ varies in the range of 0.4 mol/s to 1.7 mol/s which is equivalent to -57% to 243% of the normal operation concentration of 0.7 mol/s, respectively. However, the maximum change of the sulfuric acid molar flow rate is small, within 1 mol/s. This means that the duty of the H_2SO_4 decomposer partially transfers to the SO_3 decomposer at a lower temperature range. This effect is clearly observed from the concentration profile of SO_3 in the SO_3 decomposer. The same resonant peak of SO_3 ($W_{SO3,1}$) discharged from the SO_3 decomposer undergoes an oscillation within about $\pm 50\%$ amplitude. The resonant peak of SO_2($W_{SO2,1}$) discharged from the SO_3 decomposer has the same oscillation trend with respect to $T_{He,1}$. In the cases of $W_{H2O,1}$, $W_{H2O,2}$, $W_{SO3,2}$, $W_{H2SO4,3}$, $W_{H2O,3}$, and $W_{SO3,3}$, there is no effect of the inlet helium temperature disturbance.

4.3 Transient Responses to Inlet Helium Flow Rate Disturbance

In the same manner as in Section 4.2, the transient responses of the process stream temperature and composition to the frequency forcing function of the inlet helium flow rate were evaluated, and their results are shown in Figs. 10 and 11.

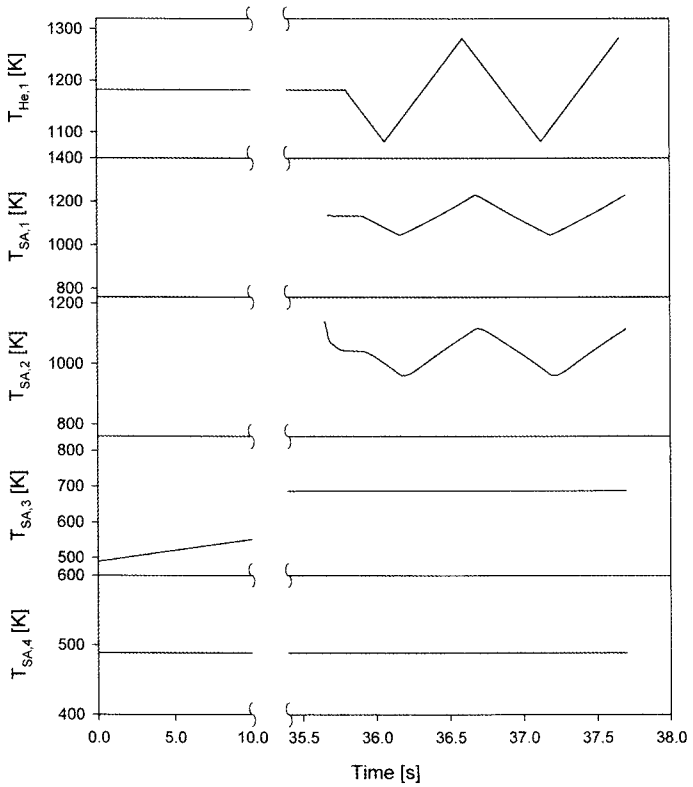

Fig. 8. Typical Response of the Process Stream Temperature to the Frequency Forcing Function of the Inlet Helium Temperature

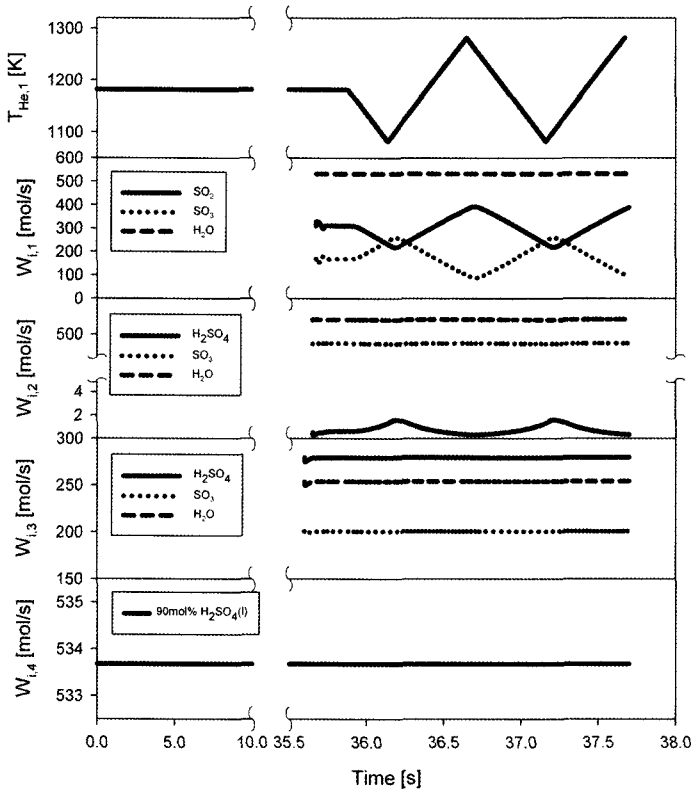

Fig. 9. Typical Response of the Process Stream Composition to the Frequency Forcing Function of the Inlet Helium Temperature

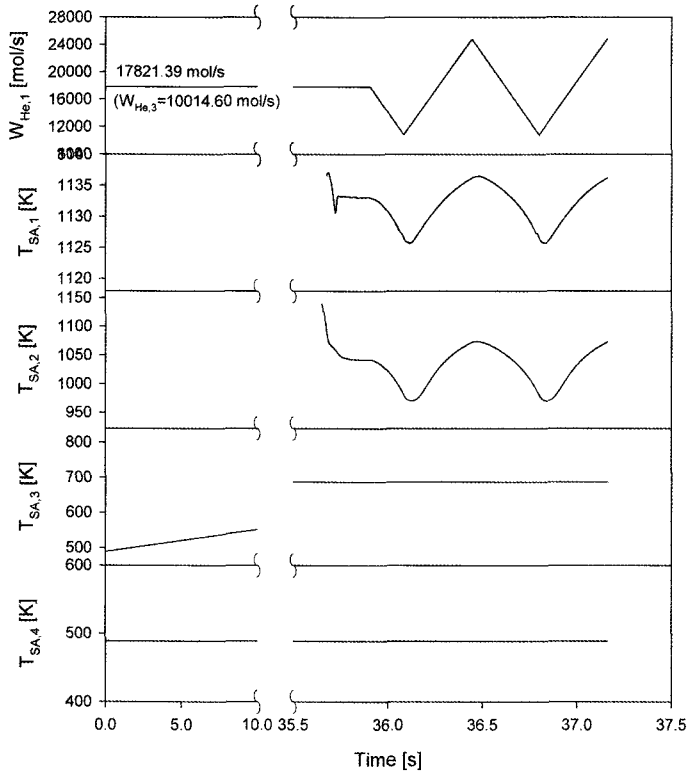

Fig. 10. Typical Response of the Process Stream Temperature to the Frequency Forcing Function of the Inlet Helium Flowrate

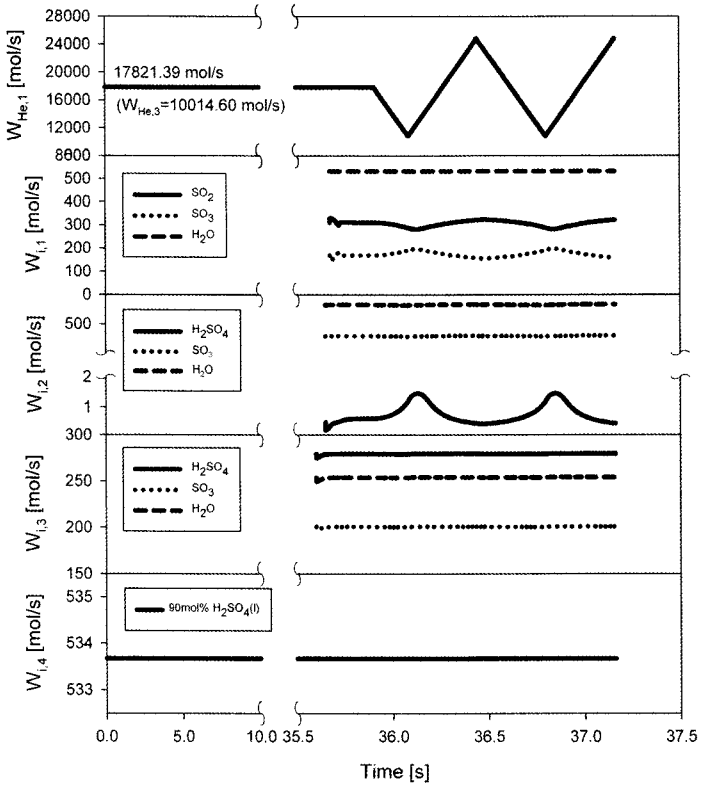

Fig. 11. Typical Response of the Process Stream Composition to the Frequency Forcing Function of the Inlet Helium Flowrate

As shown in Figs. 10 and 11, when the inlet helium flow rate ($W_{He,1}$) is changed periodically within 17,821.4 ±7,000 mol/s, which is equivalent to a ±39.3% disturbance based on the normal operation flow rate, the parameter $T_{SA,1}$ varies from 1,125.7 K to 1,136.5 K, and the parameter $T_{SA,2}$ from 970.7 K to 1,074.1 K. However, there is no variation of the temperature ($T_{SA,3}$) for the 90 mol% H_2SO_4 solution in the vaporizer. With respect to the composition, the maximum effect occurs at the sulfuric acid concentration ($W_{H2SO4,2}$) discharged from the H_2SO_4 decomposer. The amplitude of $W_{H2SO4,2}$ varies in the range of 0.4 mol/s to 1.5 mol/s which is equivalent to -57% to 214% of the normal operation concentration of 0.7 mol/s, respectively. However the maximum change of the sulfuric acid molar flow rate value is small, within 0.8 mol/s. This means that the remaining H_2SO_4 in the outlet of the H_2SO_4 decomposer due to a lower operation temperature is decomposed at the SO_3 decomposer. This effect is also clearly observed from the concentration profile of SO_3 in the SO_3 decomposer. The same resonant peak of SO_3 ($W_{SO3,1}$) discharged from the SO_3 decomposer undergoes an oscillation within about ±16.8% amplitude. The resonant peak of SO_2 ($W_{SO2,1}$) discharged from the SO_3 decomposer has the same oscillation trend as $W_{He,1}$. The effects of the inlet helium flow rate disturbance on $W_{H2O,1}$, $W_{H2O,2}$, $W_{SO3,2}$, $W_{H2SO4,3}$, $W_{H2O,3}$, and $W_{SO3,3}$ are negligibly small.

5. CONCLUSIONS

A dynamic simulation of the Second Section of an SI process has been performed to evaluate the start-up behavior and to identify the effect of the inlet helium condition changed suddenly from the normal operation temperature and flow rate on the performance of the Second Section. From the results of the start-up dynamic simulation, it is anticipated that the Second Section, which is interconnected to the helium flow and the process flow through a H_2SO_4 vaporizer, a H_2SO_4 decomposer, and a SO_3 decomposer, will approach a steady state at the same time. From the transient responses due to the changes of the inlet helium temperature and flow rate, the effect of the inlet helium temperature on the performance of the Second Section is stronger than that of the inlet helium flow rate. This means that the temperature control of the inlet helium is strictly required rather than the flow rate control of the inlet helium to keep the steady state condition in the Second Section. On the other hand, it was revealed that the changes of the inlet helium operation

conditions greatly impact the performances of SO_3 and H_2SO_4 decomposers, but have no effect on the performance of the H_2SO_4 vaporizer.

ACKNOWLEDGMENTS

This study was performed under the mid- and long-term nuclear R&D projects supported by the Ministry of Education, Science and Technology, Republic of Korea.

REFERENCES

[1] Brown L. C., Besenbruch G. E., Lentsch R. D., Schultz K. R., Funk J. F., Pickard P. S., Marshall A. C., and Showalter S. K., 2003, "High Efficiency Generation of Hydrogen using Nuclear Power". GA-A24285.

[2] Chang, J. H., Kim, Y. W., Lee, K. Y., Lee, Y. W., Lee, W. J., Noh, J. M., Kim, M. H., Lim, H. S., Shin, Y. J., Bae, K. K., and Jung, K. D., 2007, "A Study of a Nuclear Hydrogen Production Demonstration Plant," Nucl. Eng. and Technology, 39(2), pp. 1-12.

[3] Shin, Y. J., 2007, "Thermal Efficiency of EED-embedded Sulfur Iodine Cycle", KAERI Calculation Note No. NHDD-HI-CA-07-001.

[4] Sato, H., Kubo S., Sakaba, N., Ohashi, H., Sano, N., Nishihara, T., and Kunitomi, K., "Conceptual Design of the HTTR-IS Hydrogen Production System-Dynamic Simulation Code Development for Advanced Process Heat Exchanger in the HTTR-IS System", Global 2007 Proceedings, pp. 812-819, Boise, Idaho, September 9-13, 2007.

[5] Correa, D. J. and Marchetti, J. L., 1987, "Dynamic Simulation of Shell-and-Tube Heat Exchangers", Heat Transfer Engineering, 8(1), pp. 50-59.

[6] Yimin, X. and Roetzel, W., 1993, "Stationary and Dynamic Simulation of Multipass Shell and Tube Heat Exchangers with the Dispersion Model for Both Fluids", International Journal of Heat and Mass Transfer, 36(17), pp. 4221-4231.

[7] Aly, N. H. and Marwan, M. A., 1997, "Dynamic Response of Multi-effect Evaporators", Desalination, 114(2), pp. 189-196.

[8] Russell, N. T., Bakker, H. H. C., and Chaplin, R. I., 2000, "A Comparison of Dynamic Models for an Evaporation Process", Chemical Engineering Research & Design: Transactions of the Institute of Chemical Engineers, 78(8), pp. 1120-1128.

[9] Perry, Robert and Green, Don W., 1999, "Perry's chemical engineers' hand book", 7th edition, McGraw Hill, pp. 3-280 and 3-282.

[10] Roine, A., HSC Chemistry ver. 5.1, Outo Kumpu, 2002.

[11] Chopey, Nicholas P., 1994, "Handbook of Chemical engineering Calculations", Second ed., New York, McGrow Hill, pp. 7-41.

[12] Huang, C., and T-Raissi, A., 2005, "Analysis of sulfur–iodine thermochemical cycle for solar hydrogen production. Part I: decomposition of sulfuric acid", Sol Energ, 78, pp. 632–646.

[13] Fogler, H. S., 2007, "Elements of chemical reaction engineering", 4th ed., New York, Prentice Hall, pp. 110.

[14] Perry, R. H. and Chilton, C. H., 1984, "Chemical engineers' handbook", 6th ed., New York, McGraw-Hill, pp. 10-46.

[15] Perry, R. H. and Chilton, C. H., 1984, "Chemical engineers' handbook", 6th ed., New York, McGraw-Hill, pp. 5-53.